

Density fluctuations in irreversible adsorption processes: Hard ellipses in two dimensions

Zbigniew Adamczyk^{a)} and Paweł Weroński

Institute of Catalysis and Surface Chemistry, Polish Academy of Sciences, 30-239 Cracow, Niezapominajek 1, Poland

(Received 6 March 1997; accepted 2 June 1997)

Density fluctuations in 2D systems of irreversibly adsorbed particles were studied. Analytical expressions were derived connecting the magnitude of these fluctuations (characterized by the reduced variance $\bar{\sigma}^2$) with the available surface function ϕ and the isotropic pair correlation function g_0 . Limiting expansions in terms of power series of the dimensionless coverage θ were also derived. The range of validity of these expressions was determined by performing numerical simulations based on the random sequential adsorption (RSA) model. Calculations of $g_0(r)$, $g_0(s)$, ϕ , and $\bar{\sigma}^2$ were performed for hard circles and hard ellipses characterized by aspect ratio $k=2$ and 5. It was deduced that the simulation results can well be accounted for by the theoretical predictions stemming both from the RSA and equilibrium models. © 1997 American Institute of Physics. [S0021-9606(97)51233-5]

I. INTRODUCTION

Interactions of macromolecules, colloid, and bioparticles (proteins, enzymes, viruses, bacteria, etc.) with solid-liquid interface leading to adsorption and adhesion are of practical significance for polymer and colloid science, biophysics, and medicine enabling a better understanding and control of various separation processes.

In comparison with molecular system adsorption of these particles is complicated by many factors most noticeably their shape anisotropy and irreversibility due to specific interactions with the interfaces.¹⁻³ Also the external and hydrodynamic force fields may influence adsorption, especially for larger particles.⁴⁻⁷

On the other hand, the model colloidal systems are attractive for experimental studies since they can be directly observed as individual entities under an optical microscope. In this way both adsorption kinetics, pair correlation functions, and fluctuation in particle number density over various surfaces can be determined for spherically shaped particles.^{2,3,7-9} These experiments were interpreted usually in terms of theoretical approaches based on various mutations of the random sequential adsorption (RSA) model,¹⁰⁻¹² except for dense particles (of size above micrometer) for which the ballistic model was found more appropriate.^{4,5}

The essence of the RSA approach consist in assuming that particles are adsorbing sequentially and irreversibly at available surface areas at surfaces of isotropic properties; when an adsorbing particle meets an area occupied by any preadsorbed particles it is rejected; the next adsorption attempt is entirely uncorrelated with any of the previous ones. The RSA model is especially appealing because not too high surface concentrations predicts results indistinguishable from the equilibrium models, especially the available surface function (ASF) ϕ . In this way, the model colloid systems

create the unique possibility to verify by direct observations *in situ* various aspects of the statistical mechanical approaches.

In contrast to the fairly good knowledge of the RSA processes for spheres, the case of anisotropic particles has scarcely been studied. In^{13,14} adsorption of cubes (more precisely squares) and cylinders (rectangles) was investigated theoretically. Talbot *et al.*¹⁵ determined in terms of the Monte Carlo RSA simulations the jamming concentrations, and adsorption kinetics of ellipses whereas in^{16,17} similar calculations aimed at determining the ASF function and jamming concentrations for rectangles, ellipses, and spherocylinders were performed. These authors also formulated asymptotic expressions describing adsorption kinetics in the limit of low and high surface concentrations. The kinetics of adsorption of prolate spheroids (ellipses) interacting via the screened electrostatic potential was recently studied in Ref. 18.

It seems that no results are available in the literature concerning the density fluctuations in this system and their relation to the isotropic radial distribution function. This should be the goal of our paper in which we perform explicit calculations in terms of the MC-RSA model for the 2D adsorption of hard spheroids (ellipses). A comparison with equilibrium system is also carried out in order to determine the range of coincidence of density fluctuations in reversible and irreversible (RSA) systems.

II. DENSITY FLUCTUATION FORMULAE

A. Fluctuation in irreversible systems

Consider a macroscopic adsorption plane characterized by the geometrical surface area: A , much larger than particle cross-section area A_g , so the boundary effects could be neglected. Let us assume that due to some random and isotropic adsorption mechanisms a large number M of particles was accumulated at the adsorption plane. Hence the averaged

^{a)} Author to whom correspondence should be addressed. Fax: (48 12) 25 19 23. Electronic mail: nccadamcz@cyf.-kr.edu.pl

2D particle density ρ equals $M/A = \theta/A_g$, where $\theta = \rho A_g$ is the dimensionless surface concentration of adsorbed particles (coverage).

Consider now a subsystem chosen randomly somewhere at the adsorption plane whose surface area is ΔA . Denote by q the conditional probability that there are exactly N_p particles over ΔA (where $N_p \geq 0$) provided that there are M particles adsorbed over A . Obviously q should depend on N_p , M , and the ratio $\Delta A/A$. The variance of N_p is then given by the defining equation

$$\sigma^2 = \sum_{N_p \geq 0} (N_p - \langle N_p \rangle)^2 q = \langle N_p^2 \rangle - \langle N_p \rangle^2, \quad (1)$$

where $\langle N_p \rangle = \sum N_p q$ is the averaged number of particles over ΔA and $\langle \rangle$ denotes the averaging procedure.

Explicit evaluation of σ^2 requires a knowledge of q which can be calculated analytically for some Markoff processes where adsorption events are uncorrelated, i.e., particle adsorption probability at a given point is independent on preadsorbed particle positions. This would correspond to the low-density regime of irreversible RSA⁷⁻⁹ and ballistic adsorption mechanisms^{4,5} or the dilute gas model of reversible systems. In this limit q is given in the general case by the binomial distribution

$$q(N_p, M) = \binom{M}{N_p} \left(\frac{\Delta A}{A} \right)^{N_p} \left[1 - \frac{\Delta A}{A} \right]^{M-N_p}, \quad (2)$$

where

$$\binom{M}{N_p} = \frac{M!}{(M-N_p)! N_p!}$$

is the number of combinations for which particle configuration remains unchanged (undistinguishable particles).

Substituting the expression for q into Eq. (1) one can derive for σ^2 the simple formula

$$\begin{aligned} \sigma^2 &= M \frac{\Delta A}{A} \left(1 - \frac{\Delta A}{A} \right) = \rho \Delta A \left(1 - \frac{\Delta A}{A} \right) \\ &= \langle N_p \rangle \left(1 - \frac{\Delta A}{A} \right), \end{aligned} \quad (3)$$

where $\langle N_p \rangle = \rho \Delta A$ is the averaged number of particles over ΔA . Note that σ^2 does not depend explicitly on M .

In the limit when $\Delta A/A \rightarrow 0$ (while M is kept large) the binomial distribution reduces to the well-known Poisson distribution, i.e.,

$$q = p(N_p) = \frac{\langle N_p \rangle^{N_p}}{N_p!} e^{-\langle N_p \rangle}. \quad (4)$$

Using Eq. (1) one obtains $\sigma^2 = \langle N_p \rangle$ (this can also be deduced from Eq. (3) in the limit $\Delta A/A \rightarrow 0$).

As mentioned above, the Poisson distribution is expected to describe well the situation when the probability of successive adsorption events remains independent of the number of particle already present at the surface. This condition is obviously violated for larger coverages θ due to the surface exclusion effects. The adsorption probability is then gov-

erned by the available surface function (ASF) ϕ introduced by Widom¹⁹ which is equal one for $\theta=0$ and decreases to zero in irreversible (RSA) processes when the limiting (jamming) surface coverage is approached.

Exploiting the concept of ASF and using the maximum term method, it was shown in Ref. 9 that the reduced variance $\sigma^2/\langle N_p \rangle = \bar{\sigma}^2$ is given by the expression

$$\bar{\sigma}^2 = \frac{\phi}{\phi - \theta} \frac{d\phi}{d\theta} = \frac{1}{1 + \theta \frac{d\mu_{ir}/kT}{d\theta}}, \quad (5)$$

where

$$\mu_{ir} = -kT \ln \phi \quad (6)$$

can formally be treated as the irreversible potential.

One can invert Eq. (6) to calculate ϕ , i.e.,

$$\phi = e^{-\mu_{ir}/kT} = \exp \left[- \int \left(1 - \frac{1}{\bar{\sigma}^2} \right) d \ln \theta \right]. \quad (7)$$

Equation (5) is useful for calculating density fluctuations because many series expansions and interpolating functions for ϕ exist in the literature. Thus, the low-density expansions for RSA processes of convex particles assume the form^{11,18}

$$\phi = 1 - \sum_{n \geq 1} C_n \theta^n. \quad (8)$$

The $C_1 - C_3$ constants related to the virial coefficients were calculated analytically for spherical particles in 2D (disks)¹¹ and they assume the form

$$C_1 = 4, \quad C_2 = -6\sqrt{3}/\pi, \quad (9)$$

$$C_3 = 40/\pi\sqrt{3} - 176/3\pi^2 = -1.407.$$

For convex particles only C_1 can be expressed analytically²⁰ as

$$C_1 = 2 + \frac{P^2}{2\pi S_g}, \quad (10)$$

where P is the perimeter of the particle.

Ricci *et al.*¹⁷ calculated the remaining $C_2 - C_3$ coefficients numerically for ellipses, cylinders, and spherocylinders. On the other hand, the $C_1 - C_2$ constants for interacting particles (Yukawa type potential) were calculated in Ref. 18.

Substituting the series expansion Eq. (8) into Eq. (5) one can deduce that in the limit of low density the reduced variance is given by the expression

$$\bar{\sigma}^2 = 1 - C_1 \theta - 2C_2 \theta^2 - (3C_3 - C_1 C_2) \theta^3 + \dots O(\theta^4). \quad (11)$$

For low coverages this agrees with the the result of Schaaf *et al.*²¹ who deduced that $\bar{\sigma}^2 = \phi$ in the limit of low densities.

Equation (11) has a practical significance because it indicates that by measuring fluctuations in particle density (for low θ) one can determine the $C_1 = 2B_2$ constant (where B_2 is the second virial coefficient) which has a natural physical interpretation as the averaged surface area excluded by one

particle. This in turn enables one to estimate the range of interaction between adsorbed particles and adsorption kinetics (governed by ϕ) for low coverages.

B. Equilibrium systems

Since the properties of a RSA system should approach the equilibrium systems in the limit of low density, we present some useful equations characterizing fluctuations in these systems.

The variance of the density fluctuations in the grand canonical ensemble are given by the known thermodynamic relationship²²

$$\bar{\sigma}^2 = kT \frac{1}{\langle N_p \rangle} \left(\frac{\partial \mu}{\partial \langle N_p \rangle} \right)_{A,T}^{-1} = \frac{1}{\theta} \left(\frac{\partial \mu / kT}{\partial \theta} \right)_{A,T}^{-1}, \quad (12)$$

where μ is the chemical potential and T is the absolute temperature. Using the Gibbs–Duhem relationship $d\mu = (1/\rho) dp$ (where p is the 2D pressure) one can convert Eq. (12) to the useful form

$$\bar{\sigma}^2 = kT \left(\frac{\partial p}{\partial \rho} \right)^{-1} = \left(\frac{\partial \bar{p}}{\partial \theta} \right)^{-1}, \quad (13)$$

where $\bar{p} = kT p / A_g$.

Equation (13) is useful because many approximate expressions for \bar{p} as a function of θ exist, e.g., in the form of virial expansions

$$\frac{\bar{p}}{\theta} = 1 + \sum_{n \geq 2} B_n \theta^{n-1}. \quad (14)$$

By differentiating this series and substituting into Eq. (13) one obtains for $1/\bar{\sigma}^2$ the expansion

$$1/\bar{\sigma}^2 = 1 + \sum_{n \geq 2} n B_n \theta^{n-1}. \quad (15)$$

This can be inverted to the form

$$\bar{\sigma}^2 = 1 - 2B_2\theta + (4B_2^2 - 3B_3)\theta^2 + [12B_2B_3 - 4(2B_2^3 + B_4)]\theta^3 + O(\theta^4). \quad (16)$$

Since $C_2 = -2B_2^2 + \frac{3}{2}B_3$ one can deduce that this expansion is identical to the expansion Eq. (11) up to the term θ^2 .

Explicit values of B_n up to the seventh term were reported in the literature²³ for spheres (3D) and disks (2D). On the other hand, for ellipses, cylinders, and spherocylinders these virial coefficients were calculated up to the order of four only.^{17,24}

Using the scaled particle theory (SPT) Boublik²⁰ derived simple analytical expressions for the 2D pressure of arbitrary convex particles

$$\frac{\bar{p}}{\theta} = \frac{1 + (\gamma - 1)\theta}{(1 - \theta)^2}, \quad (17)$$

where $\gamma = P^2/4\pi A_g$ is the shape parameter.

By differentiating Eq. (17) with respect to θ and substituting into Eq. (13) one obtains for $\bar{\sigma}^2$ the expression

$$\bar{\sigma}^2 = \frac{(1 - \theta)^3}{1 + (2\gamma - 1)\theta}. \quad (18)$$

The low coverage expansion of Eq. (18) is

$$\bar{\sigma}^2 = 1 - 2(\gamma + 1)\theta + (8\gamma - 1)\theta^2 + 2(3 - 7\gamma)\theta^3 + \dots O(\theta)^4. \quad (19)$$

As noticed in Ref. 24, the Boublik expression for the pressure becomes rather inaccurate for elongated particles when $\gamma \gg 1$. In this case Song and Mason²⁵ proposed the following improved semiempirical equation:

$$\frac{\bar{p}}{\theta} = \frac{1 + (B_2 - 2)\theta + (1 - B_2\gamma_1)\theta^2 + B_2\gamma_2\theta^3}{(1 - \theta)^2} \quad (20)$$

where

$$\gamma_1 = 2 - \bar{B}_3 B_2,$$

$$\gamma_2 = 1 - 2\bar{B}_3 B_2 + \bar{B}_4 B_2^2,$$

$$\bar{B}_3 = B_3/B_2^2; \quad \bar{B}_4 = B_4/B_2^3.$$

Using Eqs. (20) and (13) one can derive for $\bar{\sigma}^2$ the following expression:

$$\bar{\sigma}^2 = \frac{(1 - \theta)^3}{1 + (2\gamma - 1)\theta + A_2\theta^2 + A_3\theta^3 + A_4\theta^4}, \quad (21)$$

where

$$A_2 = 3[1 - 2(1 + \gamma) + (1 + \gamma)^2 \bar{B}_3],$$

$$A_3 = -1 + 6(1 + \gamma) - 9(1 + \gamma)^2 \bar{B}_3 + 4(1 + \gamma)^3 \bar{B}_4,$$

$$A_4 = -2(1 + \gamma) + 4(1 + \gamma)^2 \bar{B}_3 - 2(1 + \gamma)^3 \bar{B}_4.$$

An implementation of Eqs. (20) and (21) one requires the third and fourth virial coefficients which have been calculated in Refs. 17 and 24.

Using the method of Ornstein and Zernicke²² one can alternatively express Eq. (13) via the two particle radial distribution function, in the commonly used form

$$\bar{\sigma}^2 = 1 + 2\pi\rho \int [g_0(\mathbf{r}) - 1] d\mathbf{r}, \quad (22)$$

where g_0 is the isotropic distribution function^{26,27} and \mathbf{r} is the center to center distance vector.

It should be mentioned that Eq. (22) is also applicable for irreversible systems, e.g., those generated in RSA processes.

III. SIMULATION METHOD

The RSA simulations were performed according to the algorithm described in some detail elsewhere.¹⁸ The basic features of the model can be characterized as

- (i) particles are placed at random over a square simulation plane ΔA with periodic conditions at its boundary; the x, y coordinates and the orientation α of the particle are sampled from uniform distributions,
- (ii) if the currently simulated particle overlaps with any

previously adsorbed it is rejected with unit probability (the Vieillard–Baron function²⁸ was used to optimize the overlapping test) and the simulation loop is repeated

- (iii) otherwise, the particle is assumed irreversibly adsorbed and its coordinates and orientation are stored.

In order to enhance the efficiency of the overlapping test a subsidiary 2D matrix was introduced containing information about numbering of neighboring particles.

The ASF function was calculated by stopping the adsorption simulation loop at a desired surface coverage, and then performing large number of virtual adsorption attempts N_{att} . Out of them only N_{succ} were potentially successful. Then, ϕ can be approximated as $N_{\text{att}}/N_{\text{succ}}$ in the limit when $N_{\text{succ}} \rightarrow \infty$. Many independent simulations of ϕ were averaged in order to increase its estimation accuracy. The derivative of ϕ needed for Eq. (7) was calculated by using subsidiary interpolating polynomials which were analytically differentiated.

The isotropic radial distribution function g_0 was calculated by generating particle populations according to the above RSA scheme and then using the definition

$$\frac{dN}{dr} = 2\pi r g_0(r) \rho, \quad (23)$$

where N is the number of neighbors separated by the distance r or less. Thus, g_0 can be calculated in practice by averaging the number of particles ΔN_p found under arbitrary orientation within the ring $2\pi r dr$ drawn around a central particle, i.e., from the formula

$$g_0(r + \Delta r/2) = \frac{1}{\rho} \left\langle \frac{\Delta N_p}{2\pi r \Delta r} \right\rangle. \quad (24)$$

Additional averages from many computer runs were taken (with particles adjacent to the simulation plane boundary rejected) in order to keep the overall number of particles considered for g_0 evaluation equal 10^5 .

As discussed in the work of Roman *et al.*²⁹ for finite particle system, the g_0 function deviates at larger distances from its infinite system counterpart by an increment inversely proportional to the total number of particles considered, i.e., about 10^{-5} in our case. This assured a sufficient accuracy of calculating $\bar{\sigma}^2$ via integration of g_0 according to Eq. (22).

Since for some application the pair distribution function expressed in terms of the surface to surface distance s has advantages over the $g_0(r)$ defined above we also calculated the isotropic $g_0(s)$ from the defining equation^{30,31} which for the 2D situation becomes

$$\frac{dN}{ds} = P_s g_0(s) \rho, \quad (25)$$

where $P_s = 2(P + \pi s)$ is the orientation averaged length of the curve formed by rotating a particle separated by the surface to surface distance s around a central particle.²⁰ The minimum surface to surface distances for a given particle

orientation was found using the method described in Ref. 18 (based on an false position solution of the nonlinear trigonometric equation).

Using $g_0(s)$ one can formulate Eq. (22) in the form

$$\bar{\sigma}^2 = 1 - C_1 \theta + \rho \int_0^\infty [g_0(s) - 1] P_s(s) ds. \quad (26)$$

The variance of particle distributions were determined in pseudo computer experiments in which particle populations of about 2×10^4 were simulated using the above RSA algorithm over the quasi macroscopic surface (the maximum coverages attained in these simulations were 0.5 since for larger values the computer time became prohibitive). Then, the large area was subdivided into square nonoverlapping subsystem having the surface area ΔA . The size of the subsystem was so adjusted that the averaged number of particles found over these areas $\langle N_p \rangle$ was approximately equal a prescribed value (we used 30, 60, 90, and 180 throughout our calculations). Averages from many computer runs were taken in order to attain the total number of subsystems equal 10^5 .

The variance of particle number found over these areas was calculated from the definition Eq. (1). For smaller coverages ($\theta < 5\%$) when the ratio $\Delta A/A$ could not be kept negligibly small a correction for the binomial distribution was introduced as described in Refs. 29 and 32.

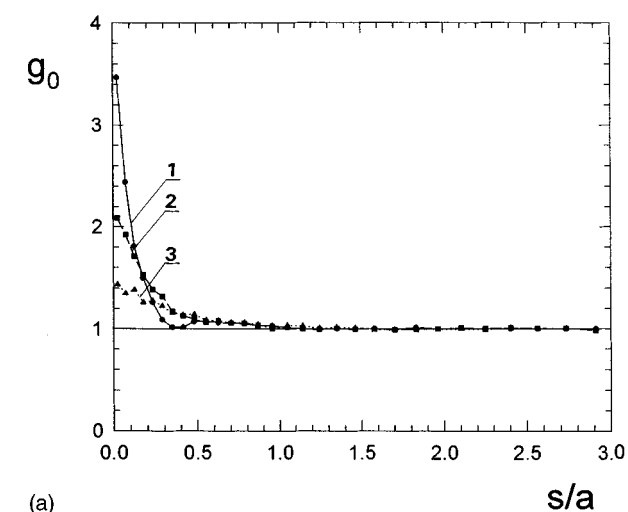
Simulations described in this work were performed for ellipses having the major semiaxis a and shorter b ; their ratio a/b is denoted by k (in previous works^{9,18} we used the parameter $A = 1/k$). All calculations have been carried out for $k = 1$ (circles), $k = 2$, and $k = 5$.

IV. RESULTS AND DISCUSSION

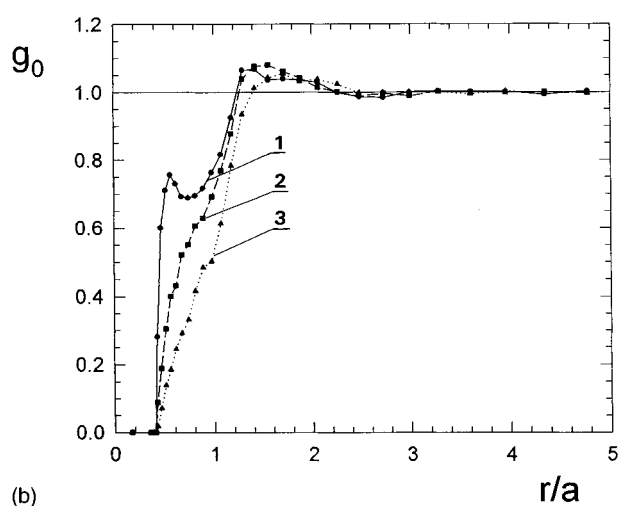
The isotropic $g_0(s)$ and $g_0(r)$ functions calculated according to the above RSA simulation method are shown in Figs. 1(a) and 1(b) for $k = 5$ and various surface coverages, i.e., 20%, 35%, and 50%. We did not attempt to compare our results with the equilibrium 2D results because these seem to not exist in the literature. As can be seen the $g_0(s)$ for elongated ellipses resembles the sphere $g(r)$ function, especially for smaller distances and low coverages. However, the minimum and the secondary peak characteristic for spheres disappeared practically in the case of ellipses. This is even more apparent when the $g_0(r)$ for ellipses are concerned [cf. Fig. 1(b)]. In this case even the first peak and hardly be distinguished and g_0 decreased almost monotonically from one to zero within a rather broad range of distances. Thus, the g_0 vs r dependencies for ellipses are considerably less informative than for spheres in respect to the nearest neighbor concentration.

In Figs. 2(a) and 2(b) the $g_0(s)$ and $g_0(r)$ functions calculated for $k = 2$, and $k = 5$ are collected. As the reference state, we plotted the corresponding g function for spheres ($k = 1$).

It should be noted that very similar results as that shown in Figs. 1 and 2 results were reported recently for spherocylinders in 2D (diskorectangles) in Ref. 27.



(a)



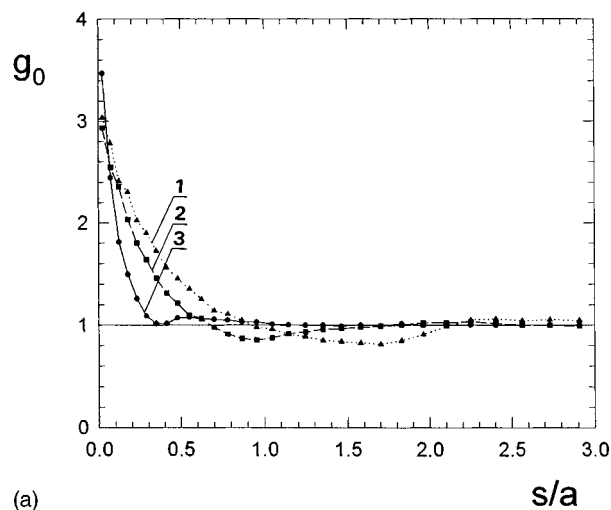
(b)

FIG. 1. (a) The pair correlation function $g_0(s)$ for hard ellipses ($k=5$) at various surface coverages: 1. $\theta=50\%$, 2. $\theta=35\%$, 3. $\theta=20\%$. (b) The pair correlation function $g_0(r)$ (hard ellipses, $k=5$), 1. $\theta=50\%$, 2. $\theta=35\%$, 3. $\theta=20\%$.

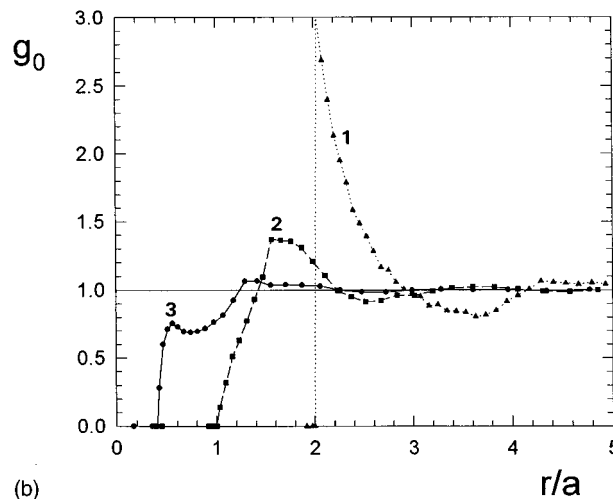
The isotropic correlation functions were used for determining the reduced variance by using Eq. (22). First it was checked if the upper integration limit r_{mx} (which must remain finite in any numerical integration) exerted any influence on the calculated $\bar{\sigma}^2$. It has been found that the integral became practically insensitive on r_{mx} when it was chosen larger than eight particle radii in the case of spheres and 2.6 major semiaxes in the case of ellipses. However, for r_{mx} larger than these limiting values a statistical scatter of $\bar{\sigma}^2$ became apparent. It should be noted that for this integration limit the number of particles within the integration area was negligibly small in comparison with the entire particle population (10^5 particles as previously stated) so the *explicit* size effects²⁸ became negligible.

It has also been proved that the integration of the $g_0(s)$ function according to Eq. (26) gave the same results as the integration of the $g_0(r)$ dependence.

The results of these calculations together with the direct determination of $\bar{\sigma}^2$ from “computer experiments” [using Eq. (1)] for hard spheres are collected in Fig. 3. As one can



(a)



(b)

FIG. 2. (a) The $g_0(s)$ function and (b) the $g_0(r)$ function for hard ellipses with various elongation. 1. $k=1$ (spheres), 2. $k=2$, 3. $k=5$, $\theta=50\%$.

notice in this Fig. the reduced variance derived from computer experiments is dependent on the averaged number of particles $\langle N_p \rangle$ adsorbed on the small area ΔA . This behavior was first detected by Senger *et al.*³² and Roman *et al.*²⁹ who attributed this to the fact that particle positions within the small area are not statistically equivalent, i.e., the entire particle population on ΔA can be divided into “core” and “peripheral” particles located close to the boundary of the small area ΔA . According to the analysis performed in Ref. 32 and 29 this leads to the increase in the variance described by two perturbing terms vanishing as $(A_g/\Delta A)^{1/2}$ and $(A_g/\Delta A)$ in the limit when $\Delta A \rightarrow \infty$. Thus, for large ΔA the reduced variance is approaching the limiting value fitted by the polynomial

$$\bar{\sigma}^2 = 1 - 4\theta + \frac{8\sqrt{3}}{\pi} \theta^2 + 0.824\theta^3 - 2.28\theta^4. \quad (27)$$

As can be noticed in Fig. 3 our simulation data (computer experiments) seem to approach for large $\langle N_p \rangle$ the values derived from Eq. (27). Also the results derived by inte-

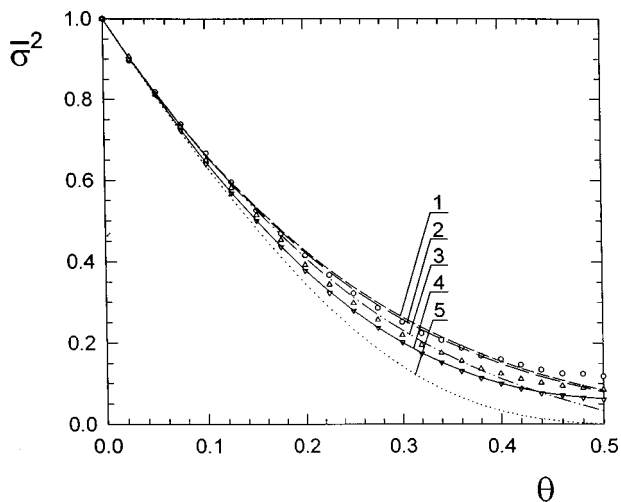


FIG. 3. The reduced variance $\bar{\sigma}^2$ as a function of θ ; open circles denote the computer experiments for $\langle N_p \rangle = 30$, triangles for $\langle N_p \rangle = 180$, inverse triangles denote the values calculated from Eq. (22) and the lines denote various analytical approximations. 1. SPT equilibrium theory (Ref. 20) Eq. (18), 2. Song Mason (Ref. 25) formula, Eq. (21), 3. Equation (5), 4. Senger *et al.* (Ref. 32) fitting polynomial Eq. (27), 5. Schaaf *et al.* (Ref. 21) formula $\bar{\sigma}^2 = \phi$.

grating the $g_0(r)$ or $g_0(s)$ functions agree very well with Eq. (27) for the entire range of surface coverages studied (0%–50%).

For comparison we also have plotted in Fig. 3 the curves derived from various analytical approximations, i.e., from Eq. (5) giving $\bar{\sigma}^2 = 1/(1 - d \ln \phi_{\text{rsa}})$, from the Schaaf *et al.*²¹ theory, i.e., $\bar{\sigma}^2 = \phi$ and from the equilibrium theory expressed by Eqs. (18) and (21). As one can notice, the variance calculated from the irreversible RSA model lies the same as θ always below that predicted for the equilibrium situation. This is understandable considering the lower probability (measured by the ASF function ϕ) of adding a particle to a RSA configuration than to the equilibrium configuration. It can also be observed in Fig. 3 that the analytical formula $\bar{\sigma}^2 = 1/(1 - d \ln \phi_{\text{rsa}})$ reflects the simulations for the entire range of θ . However, some small but statistically significant deviations occur for moderate and high coverage regions. In the latter region the positive deviations of the variance derived from computer experiments from the theoretical predictions can probably be attributed to the finite size of the large simulation area A , which should increase density fluctuations. This hypothesis could be verified by performing simulations using much larger sizes of the simulation plane A . However, due to prohibitive computer times these calculations do not seem feasible at the present.

There appears also a discrepancy between the numerical results and the theoretical predictions for moderate surface coverages which is more difficult to interpret. From the postulate that the RSA and equilibrium models give identical expressions for ϕ up to the order of θ^2 one could deduce using Eqs. (11) or (16) that the numerical results should be well fitted for low and moderate coverages by the polynomial $1 - 4\theta + 12\sqrt{3}/\pi \theta^2$ whereas in reality they are well described by the polynomial $1 - 4\theta + 8\sqrt{3}/\pi \theta^2$. This dis-

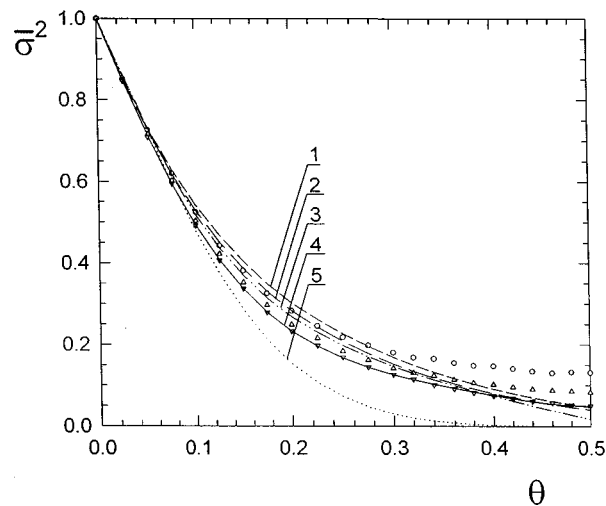


FIG. 4. Same as for Fig. 3 but for hard ellipses $k=5$. 1. SPT equilibrium theory (Ref. 20) Eq. (18), 2. Song & Mason (Ref. 25) formula, Eq. (21), 3. Equation (5), 4. Schaaf *et al.* formula (Ref. 21) $\bar{\sigma}^2 = \phi$, 5. Our fitting polynomial Eq. (29).

crepancy may suggest that in contrast to the ASF function, the RSA and equilibrium correlation $g_0(r)$ functions are different for all coverages except perhaps at the point of contact ($r \rightarrow 2a$). Indeed, by assuming

$$g_0(r) = 1 + h_1(r)\theta + O(\theta^2)$$

[where $h_1(r)$ is the first expansion coefficient of the total correlation function], one can deduce from Eq. (22) that

$$\bar{\sigma}^2 = 1 - 4\theta + H(2a)\theta^2 + O(\theta^3), \quad (28)$$

where

$$H = \frac{1}{A_g} \int_{2a}^{\infty} h_1(r)r \, dr.$$

Since the coefficient at θ^2 in the variance expression is different for RSA and equilibrium situation this proves that $h_1^{\text{rsa}} \neq h_1^{\text{eq}}$ for $r > 2a$.

Similar conclusions based on the results shown in Fig. 4 can be also formulated for elongated ellipses ($k=5$). In this case the fitting polynomial $\bar{\sigma}^2$ was found to be:

$$\bar{\sigma}^2 = 1 - 2B_2\theta + 13.98\theta^2 + 5.418\theta^3 - 58.86\theta^4 + 57.35\theta^5. \quad (29)$$

It should be mentioned in real experiments involving colloid particles the small differences between various approaches discussed above cannot be detected due to, e.g., particle polydispersity or surface heterogeneity effects. Other complicating factors are stemming from the sedimentation, diffusion, and hydrodynamic effects. However, under a certain combination of relevant physicochemical parameters the RSA case can be realized as demonstrated in recent experiments reported elsewhere⁷ involving polystyrene particles of micrometer size range adsorbing on mica from electrolyte solutions.

V. CONCLUDING REMARKS

Numerical simulations performed according to the RSA scheme revealed that the density fluctuations of nonspherical particles (ellipses) can well be described by Eq. (22) for coverage range up to 50%. The reduced variance of these fluctuations becomes identical with the equilibrium fluctuations in the limit of low coverages and can be expressed as

$$\bar{\sigma}_{\text{rsa}}^2 = \bar{\sigma}_{\text{eq}}^2 = 1 - 2B_2\theta + O(\theta)^2.$$

Hence by measuring the $\bar{\sigma}^2$ vs θ dependence for irreversible systems (colloid particles) obeying the RSA mechanism in the limit of small θ one can exactly determine the second virial coefficient of reversible systems.

However, for higher coverages θ the RSA variance is always smaller than the equilibrium variance described by Eqs. (18) and (21). The differences appear already in the third (θ^2) term of the expansion of $\bar{\sigma}^2$ vs θ . By comparison, for the ϕ vs θ expansions the differences are only apparent in the fourth- and higher-order terms. This suggests that the equilibrium and RSA total correlation functions differ even in respect to the lowest-order terms.

The irreversible fluctuations can well be reflected for the entire range of θ by Eq. (7), i.e., $\bar{\sigma}^2 = \phi / [\phi - \theta d\phi/d\theta]$ (derived by probabilistic arguments) which is also applicable for reversible systems. However, the exact value of the ϕ_{rsa} function needed in this equation must be derived from numerical simulations.

It can also be concluded that due to the limited experimental accuracy the fluctuations in irreversible colloid systems governed by the RSA model may appear identical to fluctuations in equilibrium systems for coverages up to the jamming limit.

ACKNOWLEDGMENT

This work was partly supported by the KBN Grant 3 T09 A08310.

- ¹J. Feder and T. Giaever, *J. Colloid Interface Sci.* **78**, 144 (1980).
- ²J. J. Ramsden, *Phys. Rev. Lett.* **71**, 295 (1993).
- ³Z. Adamczyk, B. Siwek, M. Zembala, and P. Belouschek, *Advances Colloid Interface Sci.* **48**, 151 (1994).
- ⁴P. Wojtaszczyk, P. Schaaf, B. Senger, M. Zembala, and J. C. Voegel, *J. Chem. Phys.* **99**, 7198 (1993).
- ⁵P. Wojtaszczyk, E. K. Mann, B. Senger, J. C. Voegel, and P. Schaaf, *J. Chem. Phys.* **103**, 8285 (1995).
- ⁶Z. Adamczyk, B. Siwek, and L. Szyk, *J. Colloid Interface Sci.* **174**, 130 (1995).
- ⁷Z. Adamczyk, B. Siwek, L. Szyk, and M. Zembala, *J. Chem. Phys.* **105**, 5552 (1996).
- ⁸Z. Adamczyk, M. Zembala, B. Siwek, and P. Warszyński, *J. Colloid Interface Sci.* **140**, 123 (1990).
- ⁹Z. Adamczyk and L. Szyk, *Bull. Pol. Ac. Chem.* **43**, 243 (1995).
- ¹⁰E. L. Hinrichsen, J. Feder, and T. Jossang, *J. Stat. Phys.* **44**, 793 (1993).
- ¹¹P. Schaaf and J. Talbot, *J. Chem. Phys.* **91**, 4401 (1989).
- ¹²J. W. Evans, *Rev. Modern Phys.* **65**, 1281 (1993).
- ¹³P. Viot and G. Tarjus, *Europhys. Lett.* **13**, 295 (1990).
- ¹⁴R. D. Vigil and R. M. Ziff, *J. Chem. Phys.* **91**, 2599 (1989).
- ¹⁵J. Talbot, G. Tarjus, and P. Schaaf, *Phys. Rev. A* **4**, 4808, (1989).
- ¹⁶P. Viot, G. Tarjus, S. M. Ricci, and J. Talbot, *J. Chem. Phys.* **97**, 5212 (1992).
- ¹⁷S. M. Ricci, J. Talbot, G. Tarjus, and P. Viot, *J. Chem. Phys.* **97**, 5219 (1992).
- ¹⁸Z. Adamczyk and P. Weroński, *Langmuir* **11**, 4400 (1995).
- ¹⁹B. Widom, *J. Chem. Phys.* **44**, 3888 (1996).
- ²⁰T. Boublik, *Molec. Phys.* **29**, 421 (1975).
- ²¹P. Schaaf, P. Wojtaszczyk, E. K. Mann, B. Senger, J. C. Voegel, and D. Bedeaux, *J. Chem. Phys.* **102**, 5077 (1995).
- ²²D. Henderson and S. G. Davison, in *Physical Chemistry, An Advanced Treatise* (Academic, New York/London, 1967), Vol. II, Chap. 7, pp. 364 and 382.
- ²³F. H. Ree and W. G. Hoover, *J. Chem. Phys.* **46**, 4181 (1967).
- ²⁴G. Tarjus, P. Viot, S. M. Ricci, and J. Talbot, *Mol. Phys.* **73**, 773 (1991).
- ²⁵Y. Song and E. A. Mason, *Phys. Rev. A* **41**, 3121 (1990).
- ²⁶W. A. Steele *J. Chem. Phys.* **57**, 1862 (1972); **58**, 3295 (1973).
- ²⁷S. M. Ricci, J. Talbot, G. Tarjus, and P. Viot, *J. Chem. Phys.* **101**, 9164 (1994).
- ²⁸J. Vieillard-Baron, *J. Chem. Phys.* **56**, 4729 (1972).
- ²⁹F. L. Roman, J. A. White, and S. Valesco, *J. Chem. Phys.* **106**, 4196 (1997).
- ³⁰B. Kumar, C. James, and G. T. Evans, *J. Chem. Phys.* **88**, 7071 (1988).
- ³¹J. Talbot, D. Kivelson, M. P. Allen, G. T. Evans, and D. Frenkel, *J. Chem. Phys.* **92**, 3048 (1990).
- ³²B. Senger, P. Schaaf, J. C. Voegel, P. Wojtaszczyk, and H. Reiss, *Proc. Natl. Acad. Sci. USA* **91**, 10029 (1994).